Crystal and magnetic structures in the Tb(Pd,Ni)Al series

2008 J. Phys.: Condens. Matter 20 104223

(http://iopscience.iop.org/0953-8984/20/10/104223)

J. Phys.: Condens. Matter **20** (2008) 104223 (7pp) doi:10.1088/0953-8984/20/10/104223

Crystal and magnetic structures in the Tb(Pd, Ni)Al series

P Javorský[1], J Prokleška[1,2], O Isnard[3] and J Prchal[1]

[1] Faculty of Mathematics and Physics, Department of Condensed Matter Physics, Charles University, Ke Karlovu 5, 121 16 Prague 2, The Czech Republic
[2] Institut Laue Langevin, 6 rue Jules Horowitz, 38042 Grenoble Cedex 9, France
[3] Institut Néel, CNRS associé à l'Université J Fourier, Boîte F, BP 166, 38042 Grenoble cedex 9, France

E-mail: javor@mag.mff.cuni.cz

Received 16 July 2007, in final form 31 August 2007
Published 19 February 2008
Online at stacks.iop.org/JPhysCM/20/104223

Abstract

We report on the magnetic structures in the $TbPd_{1-x}Ni_xAl$ compounds as determined by powder neutron diffraction. The development of magnetic structures in the Tb(Pd, Ni)Al series is relatively simple. All the compounds show the existence of two magnetic phases with almost unchanged Néel temperature $T_N \simeq 44$ K and an additional magnetic phase transition temperature $T_1 \simeq 23$ K. The arrangement of the Tb moments between T_N and T_1 is identical for all the concentrations and is characterized by a $(\frac{1}{2}, 0, \frac{1}{2})$ propagation vector with one-third of Tb moments frustrated to nearly zero. Certain concentration development occurs only below T_1. Magnetic moments that are frustrated between T_N and T_1 change their propagation below T_1 to commensurate $(\frac{1}{2}, -\frac{1}{2}, \frac{1}{2})$ or incommensurate $(\frac{1}{2}, -\tau, \frac{1}{2})$, depending on the Ni concentration. The magnetic moments stay parallel to the hexagonal c axis for all concentrations and temperatures.

1. Introduction

TbNiAl and TbPdAl belong to a large group of the RTX (R = rare earth, T = transition metal, X = p-metal) ternary compounds crystallizing in the hexagonal ZrNiAl-type structure. Among these RTX compounds, there are three groups for X = Al: RNiAl, RCuAl and RPdAl. They show various magnetic properties ranging from nonmagnetic valence fluctuators (e.g. CeNiAl [1]) to materials with complex magnetic structures, often characterized by the existence of frustrated magnetic moments (e.g. in most RNiAl compounds [2], CePdAl [3] or TmCuAl [4]). A very interesting and surprising development of magnetic behavior was observed in the $RNi_{1-x}Cu_xAl$ series with R = Tb [5], Er [6] and Dy [7]. The transition between the magnetic order in RNiAl and RCuAl is rather complex and unusual. In particular, the loss of the long-range magnetic order in the concentration range between $x \simeq 0.6$ and 0.8 was observed in all the three series. This arouses questions about the nature of exchange interactions in these materials, namely how the itinerant 3d electrons brought into the system by Ni enter in the exchange interaction game [5, 8]. Most of the previous studies have been devoted to Ni–Cu substitutions, except for an exceptional case of the Ce compounds $CePd_{1-x}Ni_xAl$ [9]. We present now a detailed neutron-diffraction study on an isoelectronic $TbPd_{1-x}Ni_xAl$ system. We expect that comparing the development of magnetism in the Ni–Cu and Ni–Pd systems (going horizontal and vertical in the periodic table) will confirm or refute presumptions [5, 8] about the magnetic exchange interactions in these materials.

Previous studies have shown that the magnetic behavior of TbNiAl and TbPdAl is rather similar. TbNiAl orders antiferromagnetically below $T_N = 45$ K and undergoes a further magnetic phase transition at $T_1 = 23$ K [10]. The magnetic order in TbNiAl is characterized by a propagation vector $(\frac{1}{2}, 0, \frac{1}{2})$ with Tb magnetic moments oriented along the c axis in both magnetic phases. One-third of the moments is strongly reduced to almost zero between T_N and T_1 [10]. TbPdAl orders antiferromagnetically below $T_N = 43$ K, with an additional phase transition at $T_1 = 23$ K [11, 12]. The propagation vectors $(\frac{1}{2}, 0, \frac{1}{2})$ and $(\frac{1}{2}, \tau, \frac{1}{2})$ were reported without further details of the magnetic structures [13]. Bulk measurements on the $TbPd_{1-x}Ni_xAl$ series indicated magnetic order in the whole series [12].

The detailed crystal-structure determination represents another subject of our study. The ZrNiAl-type structure

Table 1. Results of the refinement of the crystal structures at 60 K allowing the Ni relative occupation of both $T_{\rm I}$ and $T_{\rm II}$ sites as a free parameter. Remember that the multiplicity of the $T_{\rm II}$ site is twice the multiplicity of the $T_{\rm I}$ site. The R_B^* agreement factor corresponds to the refinement with fixed random Ni–Pd occupation on the $T_{\rm I}$ and $T_{\rm II}$ sites.

					Occupation by Ni (%)			
Ni (%)	a (pm)	c (pm)	$x_{\rm Tb}$	$x_{\rm Al}$	Site $T_{\rm I}$	Site $T_{\rm II}$	R_B (%)	R_B^* (%)
95	694.8(9)	400.3(7)	0.574(4)	0.224(9)	89(2)	98(1)	4.0	4.2
90	695.5(8)	401.3(6)	0.577(3)	0.225(8)	90(2)	90(1)	3.8	3.9
70	698.9(8)	404.4(6)	0.583(2)	0.231(6)	84(2)	63(1)	2.9	3.7
50	702.8(7)	406.5(6)	0.582(2)	0.229(6)	78(2)	36(1)	3.0	5.3
30	703.1(8)	407.1(6)	0.581(2)	0.233(3)	42(2)	24(1)	4.1	4.6
0 (A)	716.0(8)	402.1(6)	0.579(3)	0.227(9)	—	—	—	3.7
0 (B)	708.0(8)	410.9(6)	0.583(4)	0.243(9)	—	—	—	6.4

consists of two types of basal plane layer alternating along the c axis: one containing all the rare-earth atoms and one-third of the transition-metal atoms, and the other, a nonmagnetic layer formed by all the p-metal and the rest of the T atoms. Compounds crystallizing in this structure exhibit an interesting crystallographic behavior: values of the c/a ratio around 0.57 (≈0.565–0.575) are skipped as a result of an abrupt jump in the lattice parameters in the temperature or concentration dependences (see e.g. [14–16]). Both TbNiAl and TbPdAl show such a jump in their temperature dependence and, furthermore, they exhibit a coexistence of two crystallographic phases with high and low c/a in a limited temperature region [13, 15]. The x-ray absorption near-edge structure (XANES) spectra of TbPdAl revealed a relation between this structural transition and the electronic structure of Pd [17]. Several substituted Tb(Ni,Pd)Al compounds represent an exception from the general crystallographic observation: their lattice parameters fall into the 'forbidden' c/a ratio region [15]. Some kind of preferential occupation of the two crystallographic positions (within the Tb–T and Al–T planes) by Ni and Pd might help to understand this feature.

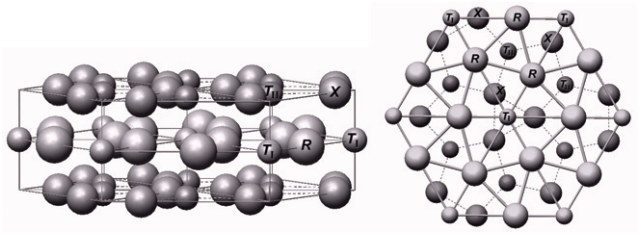

Figure 1. The hexagonal ZrNiAl-type crystal structure and its projection into the basal plane. Only the intra-plane bonds are shown in the basal-plane projection.

2. Experimental details

The polycrystalline samples were prepared by arc-melting the stoichiometric compositions of pure elements (3N for Tb, 4N5 for Ni, 5N for Al, and 3N for Pd) in a mono-arc furnace under the protection of an argon atmosphere. The samples were turned and remelted several times to achieve better homogeneity. The x-ray diffraction patterns showed single-phase samples with the hexagonal ZrNiAl-type structure.

The powder neutron-diffraction experiments were performed at the Institute Laue-Langevin, using the D1B and D1A instruments. The compounds with $x = 0.95, 0.90, 0.70$ and 0.50 were measured on D1B with a wavelength of $\lambda = 2.52$ Å over an angular range of 80° using a multidetector with a step of 0.2° between each of the 400 ^{3}He detection cells. For each compound, we collected diffraction patterns with a large statistics at 60 K (paramagnetic state), at 30 K (i.e. between $T_{\rm N}$ and $T_{\rm l}$) and at 1.8 K. Additionally, diffraction patterns with lower statistics were measured during continuous heating from 1.8 to 50 K to map the temperature development. TbPdAl and the compound with $x = 0.3$ were measured on D1A with a wavelength of $\lambda = 1.91$ Å over an angular range of 130° with a step of 0.05° using a multidetector with 25 ^{3}He counters. The diffraction patterns were collected at 6 (TbPdAl) and 12 ($x = 0.3$) different temperatures between 1.8 and 60 K. On both instruments, we used randomly oriented powder with the mass of about 4–5 g placed into the cylindrical vanadium holder with a diameter of 6 (D1B) and 12 mm (D1A). The measured data were analyzed by the Rietveld refinement method, using the FullProf program [18] with the Fermi lengths and absorption coefficients taken from [19].

3. Results

3.1. Crystal structure

TbNiAl crystallizes in the ZrNiAl-type structure, and TbPdAl crystallizes either in the same hexagonal structure or in an orthorhombic crystal structure, depending on the thermal treatment [13]. Our neutron-diffraction patterns collected in the paramagnetic state at 60 K confirmed the hexagonal ZrNiAl-type structure in the whole $TbPd_{1-x}Ni_xAl$ series. This crystal structure, shown in figure 1, consists of two types of layer at $z = 0$ and $1/2$, with the following atomic positions:

3Tb in 3(g): $(x_{\rm Tb}, 0, \frac{1}{2})$, $(0, x_{\rm Tb}, \frac{1}{2})$, $(-x_{\rm Tb}, -x_{\rm Tb}, \frac{1}{2})$

3Al in 3(f): $(x_{\rm Al}, 0, 0)$, $(0, x_{\rm Al}, 0)$, $(-x_{\rm Al}, -x_{\rm Al}, 0)$

2Ni/Pd in 2(c): $(\frac{1}{3}, \frac{2}{3}, 0)$, $(\frac{2}{3}, \frac{1}{3}, 0)$ (labeled $T_{\rm II}$)

1Ni/Pd in 1(b): $(0, 0, \frac{1}{2})$ (labeled $T_{\rm I}$).

The lattice parameters determined at 60 K are given in table 1 and shown in figure 2 together with the values obtained at 300 K from the x-ray diffraction. The values for TbPdAl and $TbPd_{0.5}Ni_{0.5}Al$ are in a good agreement with previously reported data [13, 15]. This figure documents

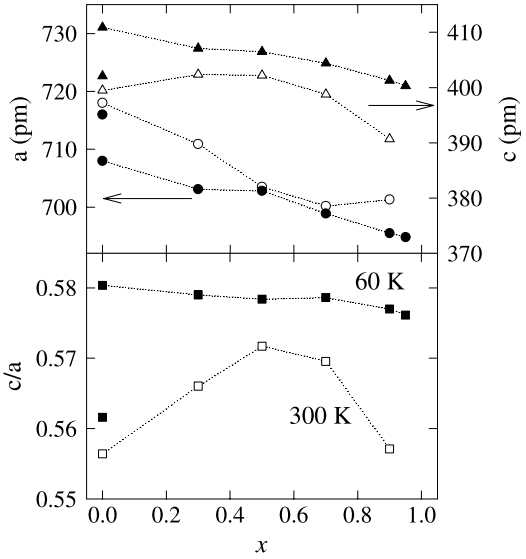

Figure 2. Concentration dependence of the lattice parameters at 60 K (black symbols, determined from neutron diffraction) and 300 K (white symbols, determined from x-ray diffraction).

the structural transition between the high-c/a and low-c/a phase that occurs in TbPdAl and TbNiAl around 110 K: when comparing the 300 and 60 K data, the value of a decreased whereas the c parameter increased. The exceptional behavior of the substituted compounds which have c/a values inside the forbidden region is also in agreement with previous results [15].

Concerning the site occupation, the analysis of the neutron-diffraction patterns at 60 K leads to a conclusion that the occupation of the T_{I} and T_{II} crystallographic sites by Ni and Pd is not random. The agreement between observed and calculated patterns improves when allowing preferential occupation on these two sites. The Ni atoms occupy the T_{I} site with a higher probability than the T_{II} site systematically for all the studied concentrations except for $x \geqslant 0.90$, where any preferential occupation hardly improves the agreement factors. The preferential occupation is most significant for compounds around $x = 0.5$, as can be seen from table 1. The atomic position parameters, x_{Tb} and x_{Al}, given in table 1 were obtained from a refinement with the preferential Ni/Pd occupation, but almost the same values are obtained with a random occupation. As already reported [13, 15], there are two crystallographic phases of TbPdAl with the same crystal structure but different lattice parameters: one phase with a low $c/a \simeq 0.56$, labeled 'A', and a second phase with a high $c/a \simeq 0.58$, labeled 'B'. The relative amount of both phases is almost the same at 60 K (A/B = 1.15). The volume fraction of phase 'A' slowly decreases with decreasing temperature but remains substantial (A/B = 0.93 at 1.8 K). The previous study of TbPdAl [13] showed a different behavior: the low-c/a phase 'A' almost vanished below 80 K. We consider this effect to be strongly sample dependent [16]; it can be influenced by annealing.

3.2. Magnetism

Previous magnetization data showed magnetic order with almost unchanged ordering temperature for the whole

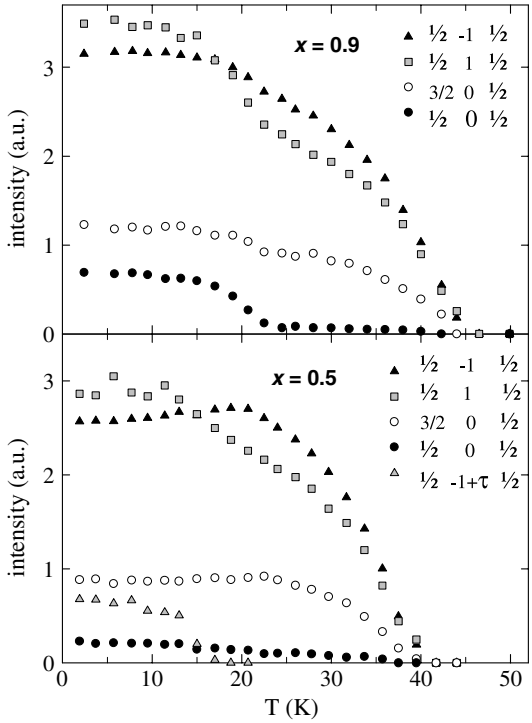

Figure 3. Temperature development of the intensities of several representative reflections for $x = 0.9$ and 0.5. The intensity of the $(\frac{1}{2}, -1+\tau, \frac{1}{2})$ peak was multiplied by a factor of three for better visibility.

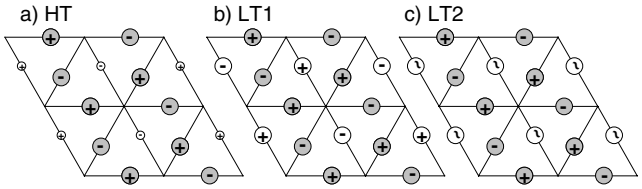

Figure 4. Determined arrangements of the Tb magnetic moments in the Tb(Pd, Ni)Al system: the high-temperature magnetic structure HT (a) and the low-temperature magnetic structures LT1 (b) and LT2 (c). See the text for details.

$TbPd_{1-x}Ni_xAl$ series [12]. Our diffraction data confirm this observation, and furthermore reveal that also the additional magnetic phase transition observed in TbNiAl and TbPdAl exists in the whole series with almost unchanged T_1. The temperature development of the magnetic intensities is illustrated in figure 3 for two representative compounds. Reflections described by the $(\frac{1}{2}, 0, \frac{1}{2})$ propagation vector appear below T_{N} for all Ni concentrations. In the low-temperature magnetic phase below T_1, we note especially a substantial increase of the $(\frac{1}{2}, 0, \frac{1}{2})$ intensity and/or appearance of reflections described by $(\frac{1}{2}, -\tau, \frac{1}{2})$, with $\tau \cong 0.12$. Let us describe now the magnetic structures in both magnetic phases.

The analysis of diffraction patterns collected around 30 K, i.e. in the high-temperature magnetic phase between T_{N} and T_1, leads to the same magnetic structure in the whole series, which is identical to that described already for TbNiAl [10] (see figure 4). All the Tb moments propagate with the

Table 2. Results of the refinement of the magnetic structures at 1.8 and 30 K.

		30 K[a]			1.8 K		
Ni (%)	Tb site	Prop. v.[b]	μ_{Tb} (μ_{B})	R_m (%)	Prop. v.[b]	μ_{Tb} (μ_{B})	R_m (%)
95	$(x, 0, \frac{1}{2}), (-x, -x, \frac{1}{2})$	**k**	7.2(2)		**k**	8.3(2)	
	$(0, x, \frac{1}{2})$	**k**	1.2(4)	7.2	**k**′	8.2(3)	4.6
90	$(x, 0, \frac{1}{2}), (-x, -x, \frac{1}{2})$	**k**	8.0(2)		**k**	8.5(2)	
	$(0, x, \frac{1}{2})$	**k**	1.3(4)	5.7	**k**′	8.3(4)	3.8
70	$(x, 0, \frac{1}{2}), (-x, -x, \frac{1}{2})$	**k**	7.4(2)		**k**	8.7(2)	
	$(0, x, \frac{1}{2})$	**k**	1.0(2)	3.4	**k**′	5.4(6)	4.8
50	$(x, 0, \frac{1}{2}), (-x, -x, \frac{1}{2})$	**k**	7.6(2)		**k**	8.4(2)	
	$(0, x, \frac{1}{2})$	**k**	1.4(3)	3.4	**k**′	2.3(1.2)	4.1
	$(0, x, \frac{1}{2})$				**k***	7.0(5)	9.3
30	$(x, 0, \frac{1}{2}), (-x, -x, \frac{1}{2})$	**k**	6.4(2)		**k**	8.5(2)	
	$(0, x, \frac{1}{2})$	**k**	1.2(3)	3.8	**k**′	1.8(1.2)	3.7
	$(0, x, \frac{1}{2})$				**k***	7.7(4)	9.8
0 (A)	$(x, 0, \frac{1}{2}), (-x, -x, \frac{1}{2})$	**k**	6.5(2)		**k**	8.4(3)	
	$(0, x, \frac{1}{2})$	**k**	1.2(3)	5.8	**k**′	7.8(8)	4.3
0 (B)	$(x, 0, \frac{1}{2}), (-x, -x, \frac{1}{2})$	**k**	6.5(2)		**k**	8.4(3)	
	$(0, x, \frac{1}{2})$	**k**	1.2(3)	5.8	—	0.0	3.7
	$(0, x, \frac{1}{2})$				**k***	8.8(6)	11.3

[a] Nominal value; the real sample temperature ranged between 27 and 30 K.

[b] We use the following notation for the propagation vectors: $\mathbf{k} = (\frac{1}{2}, 0, \frac{1}{2})$, $\mathbf{k}' = (\frac{1}{2}, -\frac{1}{2}, \frac{1}{2})$ and $\mathbf{k}^* = (\frac{1}{2}, -\tau, \frac{1}{2})$ with $\tau \cong 0.12(1)$.

same propagation vector $\mathbf{k} = (\frac{1}{2}, 0, \frac{1}{2})$ but they are not of the same magnitude. The moments at $(0, x_{\mathrm{Tb}}, \frac{1}{2})$ have significantly smaller magnitude than the remaining two-thirds of the moments at $(x_{\mathrm{Tb}}, 0, \frac{1}{2})$ and $(-x_{\mathrm{Tb}}, -x_{\mathrm{Tb}}, \frac{1}{2})$. The values obtained for individual compositions are given in table 2. We shall note that this magnetic structure can be identified with a moment arrangement derived by the representation analysis [10] if the reduced Tb moments at $(0, x_{\mathrm{Tb}}, \frac{1}{2})$ are equal to zero. Such a model with fixed zero moments gives rather worse agreement with the observed intensities ($R_m \simeq 9\%$).

In the low-temperature magnetic phase (i.e. below T_1), the antiferromagnetic chain formed by the Tb moments at $(x_{\mathrm{Tb}}, 0, \frac{1}{2})$ and $(-x_{\mathrm{Tb}}, -x_{\mathrm{Tb}}, \frac{1}{2})$ sites remains the same as above T_1. The remaining one-third of the moments at $(0, x_{\mathrm{Tb}}, \frac{1}{2})$, that are strongly reduced above T_1, change their propagation and form generally two types of structures depending on the Ni concentration. The first type, labeled LT1 in figure 4, is identical to the magnetic structure of TbNiAl [10]: the Tb moments at $(0, x_{\mathrm{Tb}}, \frac{1}{2})$ propagate with $\mathbf{k}' = (\frac{1}{2}, -\frac{1}{2}, \frac{1}{2})$ or $(0, \frac{1}{2}, \frac{1}{2})$ that are both equivalent to **k** in the hexagonal symmetry. All the Tb moments are aligned along the c axis and are of the same magnitude. In the other type of structure, labeled LT2 in figure 4, Tb moments at $(0, x_{\mathrm{Tb}}, \frac{1}{2})$ propagate incommensurately with $\mathbf{k}^* = (\frac{1}{2}, -\tau, \frac{1}{2})$. They are aligned also along the c axis and form a sine-wave amplitude modulated chain.

There is no sharp transition between the LT1 and LT2 magnetic structure in the concentration dependence. The first structure is adopted by compounds with a large Ni content ($x = 0.95, 0.90$). On decreasing the Ni content, the LT2 structure develops and both types of propagation on the $(0, x_{\mathrm{Tb}}, \frac{1}{2})$ site coexist. We observe this first for the $x = 0.70$ compound: the ordered commensurate moment decreases and the intensities described by $\mathbf{k}^*$ show themselves for example as a broadening of the $(\frac{1}{2}, 0, \frac{1}{2})$ reflection (see figure 5). The incommensurate LT2 structure already clearly dominates in the $x = 0.50$ compound, and the LT1 structure is practically suppressed for 30% Ni (see table 2).

The case of pure TbPdAl is more complex because of the two crystallographic phases. The refinement of the 1.8 K data reveals that the low-c/a phase 'A' orders purely with the LT1 structure, whereas the high-c/a phase 'B' orders purely with the LT2 structure. In addition to the described magnetic structures, there are in TbPdAl small magnetic intensities described by $(0, 0, 0)$ propagation (see the (100) peak in figure 6). They appear already below T_{N} and stay almost constant down to 1.8 K. These intensities are too small to refine the corresponding magnetic arrangement unambiguously. The magnitudes of the Tb moments on different sites at 1.8 K (see table 2) indicate that it might be related to a ferromagnetic component on the $(0, x, \frac{1}{2})$ site of the 'A' crystallographic phase. Such a model gives a reasonable agreement with the observed data, and we obtain a moment of $\simeq 1.2\mu_{\mathrm{B}}$ parallel to the c axis.

All the parameters of the determined magnetic structures are summarized in table 2. Our final fits were obtained assuming zero moments on Ni or Pd atoms. Allowing these moments does not bring any improvement of the fit, similar

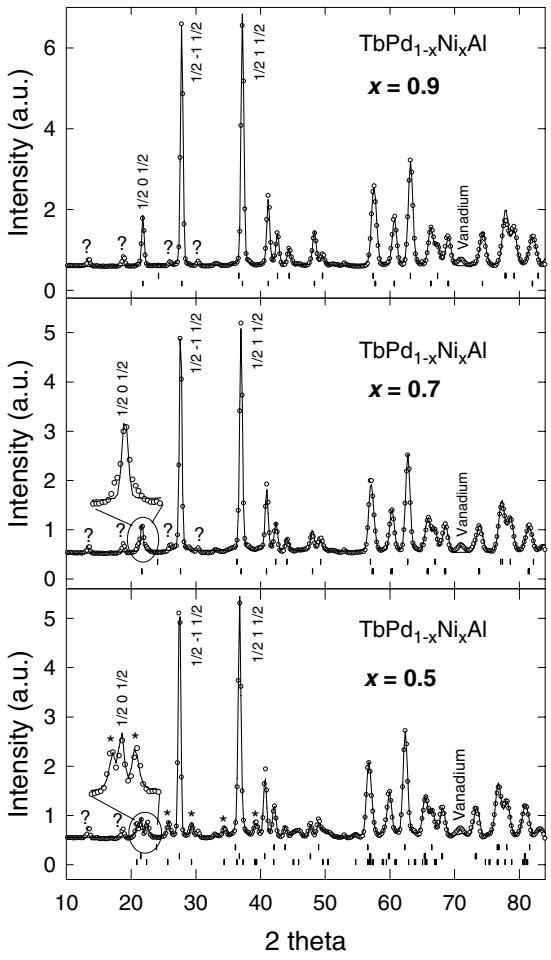

Figure 5. The diffraction patterns of $TbPd_{1-x}Ni_xAl$ for $x = 0.9$, 0.7 and 0.5 at 1.8 K, obtained on D1B with $\lambda = 2.52$ Å. The solid lines represent the fit with models described in the text, the '*' mark the most intense reflections belonging to the $(\frac{1}{2}, -\tau, \frac{1}{2})$ propagation, and the '?' mark the magnetic impurity peaks. The vertical marks below the data denote all nuclear and magnetic reflections.

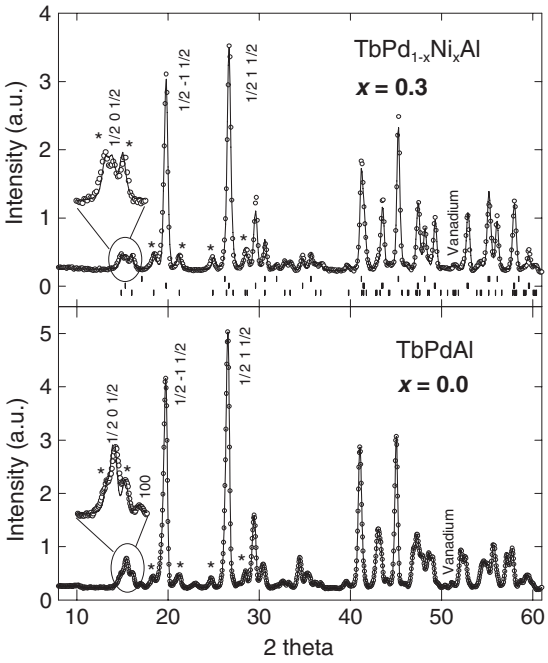

Figure 6. The diffraction patterns of $TbPd_{1-x}Ni_xAl$ for $x = 0.3$ and 0.0 (=TbPdAl) at 1.8 K, obtained on D1A with $\lambda = 1.91$ Å. The solid lines represent the fit with models described in the text, and the '*' mark the most intense reflections belonging to the $(\frac{1}{2}, -\tau, \frac{1}{2})$ propagation. The vertical marks below the data denote all nuclear and magnetic reflections (not shown for TbPdAl because of the too large number of reflections in the two-phase sample).

to previous studies on TbNiAl or other RTX compounds with T = Ni (see e.g. [2, 10, 20]). The agreement factors R_m are relatively high for the incommensurate magnetic phase because the corresponding intensities are relatively small and overlap with other higher peaks.

Besides the nuclear and magnetic intensities of the Tb(Pd, Ni)Al phase, we observe also small additional peaks in the 1.8 K pattern (see figure 5) for $x = 0.95$, 0.9, 0.7 and 0.5. They are centered at 2θ positions of 8.8°, 13.5°, 18.8° and 30.4° (corrected for zero shift). The temperature dependence of the diffraction pattern reveals that they all appear below $\simeq$18 K. They appear exactly on the same 2θ values for all mentioned Ni concentrations x, thus independently of the lattice parameters of the investigated Tb(Pd, Ni)Al compounds. This indicates that they do not belong to the main phase investigated. We ascribe these peaks to an impurity phase which has relatively weak nuclear peaks not seen in the x-ray patterns at 300 K nor in the neutron-diffraction patterns at 30 or 60 K but with strong magnetic intensities that appear below the ordering temperature ($\simeq$18 K) of this phase. We believe that the presence of a small amount of this impurity phase does not influence the intrinsic properties of the compounds studied. Such an opinion is corroborated by the fact that the $x = 0.95$ and 0.90 compounds exhibit expected magnetic properties identical to those of TbNiAl.

4. Discussion

We discuss first the crystal structure. As mentioned in the introduction, the $TbPd_{1-x}Ni_xAl$ compounds represent a certain exception from the general rule about the forbidden c/a ratio of the lattice parameters. Instead of a large jump of the c and a values that results in a jump of the c/a from $\approx$0.565 to 0.575, these substituted compounds show a smooth transition, with c/a values even inside the forbidden range (see also figure 2). We believe that it is due to a structural disorder in these materials. Our study shows certain preferential occupation on the T-sites by Ni/Pd atoms but still with a large degree of randomness. Taking into account relatively different size of the Ni and Pd atoms, this leads to variable geometry of the bonds. The forbidden c/a then can be realized. It is different from the Ni–Cu substitution in R(Ni, Cu)Al systems, where we substitute atoms with similar size. No preferential occupation is observed in these compounds, and a sharp c/a jump occurs like in many non-substituted materials [16].

Let us now turn to the magnetic properties. The development with the Ni–Pd substitution is very simple. The ordering temperatures remain almost unchanged, and

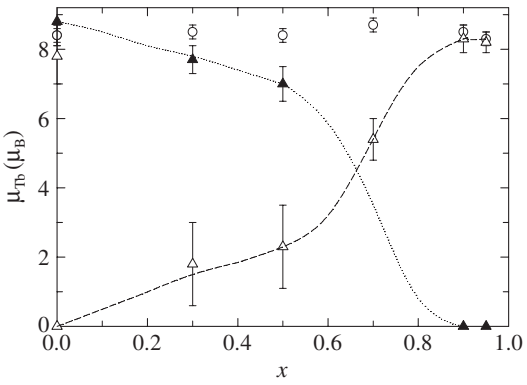

Figure 7. Concentration dependence of the Tb magnetic moments as obtained from our refinements at 1.8 K: circles denote moments at the $(x, 0, \frac{1}{2})$ and $(-x, -x, \frac{1}{2})$ sites, and white (black) triangles denote the commensurate (incommensurate) moments at the $(0, x, \frac{1}{2})$ site. The incommensurate moment for $x = 0.7$ could not be refined with reasonable precision. The lines are only to guide the eye; in TbPdAl they point to the moment observed in the high-c/a phase 'B' (see the text and table 2 for more details).

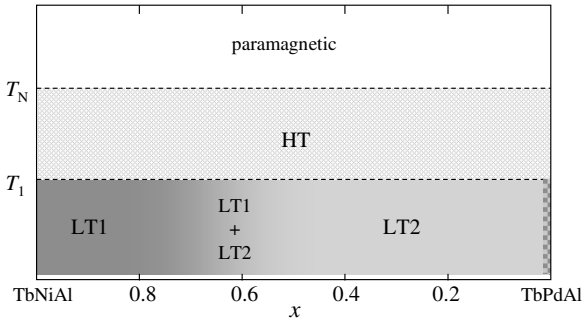

Figure 8. Schematic picture of the development of magnetic structures in the Tb(Pd, Ni)Al system. HT stands for the high-temperature magnetic structure, and LT1 and LT2 denote the low-temperature magnetic structures shown in figure 4, respectively. Both LT1 and LT2 are observed in TbPdAl, depending on the crystallographic phase.

two-thirds of the Tb moments remain completely untouched by the substitution (see table 2 and figure 7). The only parameter influenced is the change of propagation between commensurate and incommensurate nature of the remaining one-third of moments below T_1 as documented in figures 7 and 8. The uniaxial anisotropy is also conserved. Such a simple behavior is in a strong contrast to very complex development observed in the R(Ni, Cu)Al compounds [5–8]. The main difference between both types of substitution lies in the fact that Ni and Pd are isoelectronic, whereas Cu atoms bring one additional electron. The comparison between Tb(Pd, Ni)Al and R(Ni, Cu)Al confirms that the magnetic behavior is primarily driven by the density of conduction electrons that mediate the R–R exchange interaction (in fact the RKKY-type). The change of interatomic distances, that is relatively large in Tb(Pd, Ni)Al, plays a secondary role.

The magnetic structures in $TbPd_{1-x}Ni_xAl$ compounds with high Pd content ($x = 0.1$, 0.2, 0.4) were studied by Dönni *et al* [21] simultaneously with our work. The results of both independent studies are in a good agreement. All three Pd-rich compounds show magnetic structures identical to the LT2 arrangement in figure 4, i.e. the same as for $x = 0.3$ in our study. More interesting are the results on pure TbPdAl. The low-c/a crystallographic phase prefers the LT1 structure, whereas the high-c/a phase orders in the LT2 structure. The LT2 arrangement was also reported on a TbPdAl sample that was single-phase (high c/a) at low temperatures [13, 21], which is consistent with our results. This might lead to an idea that the c/a ratio is the key point that influences whether the LT1 or LT2 magnetic structure will occur. In that case, all $TbPd_{1-x}Ni_xAl$ compounds would show the LT2 arrangement because their crystal structure at low temperatures is identified with the high-c/a phase. But it contradicts our results: the Ni-rich part prefers the LT1 structure despite the high c/a value.

Our study corroborates previous conclusions about the magnetic behavior in this family of RTX compounds: the exchange interactions leading to the magnetic order in these compounds can be influenced by subtle changes of the electronic parameters (via electron density at the Fermi level) or crystal structure (via interatomic distances). These are typical features of the RKKY interactions that are expected to play the key role here since the transition metal does not carry an ordered magnetic moment. We shall note here that in the case of TbNiAl strong ferromagnetic interactions are present as well, and the whole antiferromagnetic order can be very easily turned to ferromagnetic by applying a small magnetic field [10, 22] or by a few per cent substitution of Ni by Cu [5] or Tb by Y [23]. Single-crystal studies are highly desirable for further investigations of these compounds.

5. Conclusions

We have investigated the crystal and magnetic structures in the $TbPd_{1-x}Ni_xAl$ compounds. The crystal-structure refinement reveals that the Ni atoms occupy preferably the 1(b) site within the R–T plane, whereas the Pd atoms occupy more the 2(c) sites. The development of the magnetic behavior is rather simple. There are two magnetic phases for all the investigated compositions with almost unchanged transition temperatures $T_N \simeq 44$ K and $T_1 \simeq 23$ K. The Tb moments are aligned along the c axis. Two-thirds of the moments form an antiferromagnetic chain and do not change with temperature or Ni concentration. The remaining one-third of moments is highly frustrated between T_N and T_1 and changes propagation between commensurate and incommensurate below T_1, depending on the Ni concentration. Such a simple development is in a contrast to very complex behavior observed in the R(Ni, Cu)Al compounds.

Acknowledgments

The work was supported by the Grant Agency of the Czech Republic under the Grant No. 202/06/0178 and is a part of the research program MSM 0021620834 financed by the Ministry of Education of the Czech Republic. We would also like to acknowledge the ILL for the beam time allocation and support during the measurement.

References

[1] Bandyopadhyay B, Ghoshray K, Ghoshray A and Chatterjee N 1988 *Phys. Rev.* B **38** 8455
[2] Ehlers G and Maletta H 1996 *Z. Phys.* B **101** 317
[3] Dönni A, Ehlers G, Maletta H, Fischer P, Kitazawa H and Zolliker M 1996 *J. Phys.: Condens. Matter* **8** 11213
[4] Javorský P, Gubbens P C M, Mulders A M, Prokeš K, Stüsser N, Gortenmulder T J and Hendrikx R W A 2002 *J. Magn. Magn. Mater.* **251** 123
[5] Ehlers G, Ahlert D, Ritter C, Miekeley W and Maletta H 1997 *Europhys. Lett.* **37** 269
[6] Prchal J, Javorský P, Sechovský V, Dopita M, Isnard O and Jurek K 2004 *J. Magn. Magn. Mater.* **283** 34
[7] Prchal J, Javorský P, Detlefs B, Daniš S and Isnard O 2007 *J. Magn. Magn. Mater.* **310** 589 (erratum)
[8] Prchal J, Javorský P, Dopita M, Isnard O and Sechovský V 2006 *J. Alloys Compounds* **408–412** 155
[9] Isikawa Y, Kuwai T, Mizushima T, Abe T, Nakamura G and Sakurai J 2000 *Physica* B **281/282** 365
[10] Javorský P, Burlet P, Sechovský V, Andreev A V, Brown J and Svoboda P 1997 *J. Magn. Magn. Mater.* **166** 133
[11] Kitazawa H, Dönni A and Kido G 2000 *Physica* B **281/282** 165
[12] Kitazawa H, Eguchi S and Kido G 2003 *Physica* B **329–333** 1053
[13] Dönni A, Kitazawa H, Fischer P and Fauth F 1999 *J. Alloys Compounds* **289** 11
[14] Kusz J, Böhm H, Talik E, Skutecka M and Deniszczyk J 2003 *J. Alloys Compounds* **348** 65
[15] Prchal J, Kitazawa H, Furubayashi T, Javorský P, Koyama K and Sechovský V 2006 *Physica* B **378–380** 1102
[16] Prchal J, Javorský P, Kitazawa H, de Boer F R, Diviš M, Rusz J, Dönni A, Daniš S and Sechovský V 2007 *Phys. Rev.* B submitted
[17] Mizumaki M, Yoshii K, Kitazawa H and Tanida H 2003 *J. Solid State Chem.* **171** 291
[18] Rodriguez-Carvajal J 1993 *Physica* B **192** 55
[19] Sears V F 1992 *Neutron News* **3** 26
[20] Szytuła A, Penc B and Ressouche E 1996 *J. Alloys Compounds* **244** 94
[21] Dönni A, Keller L, Kitazawa H, Prchal J and Fischer P 2007 *J. Alloys Compounds* submitted
[22] Ehlers G, Ritter C, Stewart J R, Hillier A D and Maletta H 2007 *Phys. Rev.* B **75** 024420
[23] Ehlers G, Ritter C, Kurtjakow A, Miekeley W, Stüsser N, Zeiske Th and Maletta H 1999 *Phys. Rev.* B **59** 8821